Bull. Mater. Sci., Vol. 35, No. 6, November 2012, pp. 1011–1017. © Indian Academy of Sciences.

Synthesis and luminescence properties of $BaTiO_3$:RE (RE = Gd^{3+}, Dy^{3+}, Tb^{3+}, Lu^{3+}) phosphors

ESRA KORKMAZ[†] and NILGUN OZPOZAN KALAYCIOGLU*
Department of Chemistry, Faculty of Science, Erciyes University, 38039 Kayseri, Turkey
[†]Department of Chemistry, Faculty of Science and Arts, Bozok University, 66200 Yozgat, Turkey

MS received 18 October 2011; revised 7 February 2012

Abstract. **Gd^{3+}, Dy^{3+}, Tb^{3+} and Lu^{3+} doped $BaTiO_3$-based phosphors were synthesized with modified solid-state technique at 1000 °C. The optimization of reaction conditions were carried out by thermogravimetry and differential thermal analysis methods (DTA/TG). The reaction products obtained in an air atmosphere were characterized by X-ray powder diffraction (XRD). Surface and elemental analyses were performed by using an SEM instrument. The excitation and emission spectra were recorded by photoluminescence spectrophotometer (PL). The thermoluminescence (TL) properties of $BaTiO_3$ samples doped with Gd^{3+}, Dy^{3+}, Tb^{3+} and Lu^{3+} were investigated.**

Keywords. **Solid-state reaction; perovskite oxide phosphors; luminescence; XRD; SEM; DTA/TG.**

1. Introduction

Rare earth (RE)-doped phosphors have been intensively applied in luminescent and display devices (Shionoya and Yen 1999). In 1995, Bhargava *et al* reported that the radiative transition rate of ZnS:Mn nanocrystals increased 5-fold in comparison with that of the bulk. Despite the fact that this result was strongly criticized later, studies on the fluorescence (light emission from the materials while it is irradiated by light) properties of RE-doped nanophosphors, such as electronic transitions (Meltzer *et al* 1999, 2002; Wuister *et al* 2004), confinement on energy transfer (Liu *et al* 2002, 2003), and surface effects (Tissue 1998; Williams *et al* 1998; Yan *et al* 2003; Lehmann *et al* 2004), have attracted great interest. Among these properties, surface defects have attracted intensive attention as a major factor affecting the fluorescence efficiency of nanosized phosphors. Generally, surface defects are regarded as a bad factor to the nanophosphors because they quench the luminescence efficiency of conventional phosphors (Tissue 1998). Nevertheless, in phosphorescence (light emission that persists after the cessation of excitation) materials, defects acting as traps of energy storage benefit phosphorescence emission (Matsuzawa *et al* 1996; Qiu *et al* 2001; Clabau *et al* 2005, 2006; Liu *et al* 2005). To improve the phosphorescence intensity and persistent time, increase of density of traps in these materials is needed (Jia *et al* 2002).

In this paper, $BaTiO_3$, $BaTiO_3$:Gd^{3+}, $BaTiO_3$:Dy^{3+}, $BaTiO_3$:Tb^{3+} and $BaTiO_3$:Lu^{3+} were synthesized by a modified solid-state reaction at 1000 °C. The thermal behaviour, crystal structure, photoluminescence properties, thermoluminescence properties and morphological characterization were investigated.

2. Experimental

$BaTiO_3$:RE (RE = Gd^{3+}, Dy^{3+}, Tb^{3+} and Lu^{3+}) phosphors were synthesized by a modified solid-state reaction. All the starting materials, $Ba(NO_3)_2$ (99%), $Ti(OC_4H_9)_4$ (99%), $Gd(NO_3)_3{\cdot}H_2O$ (99·99%), $Dy(NO_3)_3{\cdot}5H_2O$ (99·99%), $Tb(NO_3)_3{\cdot}6H_2O$ (99·99%) and $Lu(NO_3)_3{\cdot}XH_2O$ (99·99%) were weighed according to the nominal composition of $BaTiO_3$, $(Ba_{0.90}Gd_{0.01})TiO_3$, $(Ba_{0.90}Dy_{0.01})TiO_3$, $(Ba_{0.90}Tb_{0.01})TiO_3$ and $(Ba_{0.90}Lu_{0.01})TiO_3$. These mixtures were ground homogeneously by an agate mortar at room temperature for 2 h. The hydrolysis of $Ti(OC_4H_9)_4$ started immediately during the grinding process, accompanied by the evaporation of butyl alcohol. As the reaction proceeded, the mixture became mushy and underwent gradual changes in colour, from transparent to white. A white sample was thus obtained. Eventually, ultrafine white powders were produced after calcinations at the following temperatures: at 600 °C for 2 h, 900 °C for 6 h and 1000 °C for 2 h.

DTA/TG combined system (PERKIN ELMER Diamond, USA) was used to determine the reaction conditions in the temperature range 50–1200 °C under an inert N_2 atmosphere with a heating rate of 10°C/min.

Structural characterization was analysed by X-ray diffraction (XRD; Bruker AXS D8) spectra with CuKα line of 1·5406 Å. Scanning electron microscopy (SEM) images and EDX analysis were taken with a LEO 440 model scanning electron microscope using an accelerating voltage of 20 kV.

*Author for correspondence (nozpozan@erciyes.edu.tr)

Excitation and emission spectra of the phosphors were recorded by a Perkin Elmer LS 45 model luminescence spectrophotometer with xenon lamb.

The thermoluminescence (TL) glow curve of phosphors were measured by using a TL reader (Harshaw-QS 3500, Erlangen, Germany) at a linear heating rate of 1 °C/s up to 200 °C after irradiation using a $^{90}Sr/^{90}Y$ β-source (2·2 MeV) at a dose rate of ∼0·04 Gy/s at *RT*.

3. Results and discussion

3.1 *Characterization of phosphor*

Five different phosphor samples were investigated in this paper. Figure 1 illustrates DTA/TG curves of nominal composition, $BaTiO_3$.

The mixture obtained by the modified solid-state reaction incurs a mass loss in the ratio of 22% between 50 °C and 500 °C and, at this range, one endothermic peak is observed. These thermal behaviours correspond to the disintegration of the butyl alcohol from the medium. The main weight loss of 20% observed at 597 °C indicates decomposition of $Ba(NO_3)_2$ which is transformed into BaO. This means that the decomposition is almost complete and the crystallization of $BaTiO_3$ occurs at 600 °C.

3.2 *Phase formation and particle size analysis*

XRD patterns of $BaTiO_3$ and $BaTiO_3$:RE (RE = Gd^{3+}, Dy^{3+}, Tb^{3+}, Lu^{3+}) calcined at 1000 °C are shown in figure 2. XRD patterns for these $BaTiO_3$:RE phosphors were measured which showed a similar crystalline system. The XRD patterns in figure 2 were also found to be in good agreement with those of $BaTiO_3$ listed in JCPDS card files #05-0626: tetragonal; $a = 399{\cdot}4$, $c = 403{\cdot}8$ pm. All of the patterns are in agreement with the tetragonal crystal system known from bulk $BaTiO_3$ ($a = 400{\cdot}90$ and $c = 400{\cdot}28$ pm).

SEM micrographs of $BaTiO_3$: RE (RE = Gd^{3+}, Dy^{3+}, Tb^{3+}, Lu^{3+}) phosphors are shown in figure 3. The obtained micrographs show that the particles agglomerate and the average grain size diameter is in the range of 250–300 nm. The elemental analysis of the synthesized products was performed using energy dispersive X-ray analysis (EDX) technique, which can be used with SEM system when desired. The measured patterns are presented in figure 4. EDX analysis of the chemical composition of phosphors confirms the results of the experimental work. EDX analysis results of phosphors are listed in table 1.

3.3 *Luminescence properties*

The excitation and emission spectra obtained for $BaTiO_3$: RE (RE = Gd^{3+}, Dy^{3+}, Tb^{3+}, Lu^{3+}) are shown in figures 5 and 6. $BaTiO_3$ is seen as a broad, excitation band ranging from 270–300 nm with a maximum at about 280 nm. $BaTiO_3$:1%Dy^{3+} and $BaTiO_3$:1%Lu^{3+} is seen as an excitation band ranging from 260–290 nm with a maximum at about 275 nm. $BaTiO_3$:1%Gd^{3+} is seen as an excitation band ranging from 275–310 nm with a maximum at about 290 nm. In the excitation spectra of $BaTiO_3$:1%Gd^{3+}, there is one excitation band from 210 nm to 240 nm with a maximum at about 220 nm.

Obviously, the excitation spectrum of $BaTiO_3$ band is ascribed to a charge transfer from the oxygen ligands to the central titanium atom. The valence-conduction band transition from Ti^{4+}–O^{2-} to Ti^{3+}–O^{-} is seen to occur (Ruza *et al* 1998). The addition of RE^{3+} atoms increased the excitation

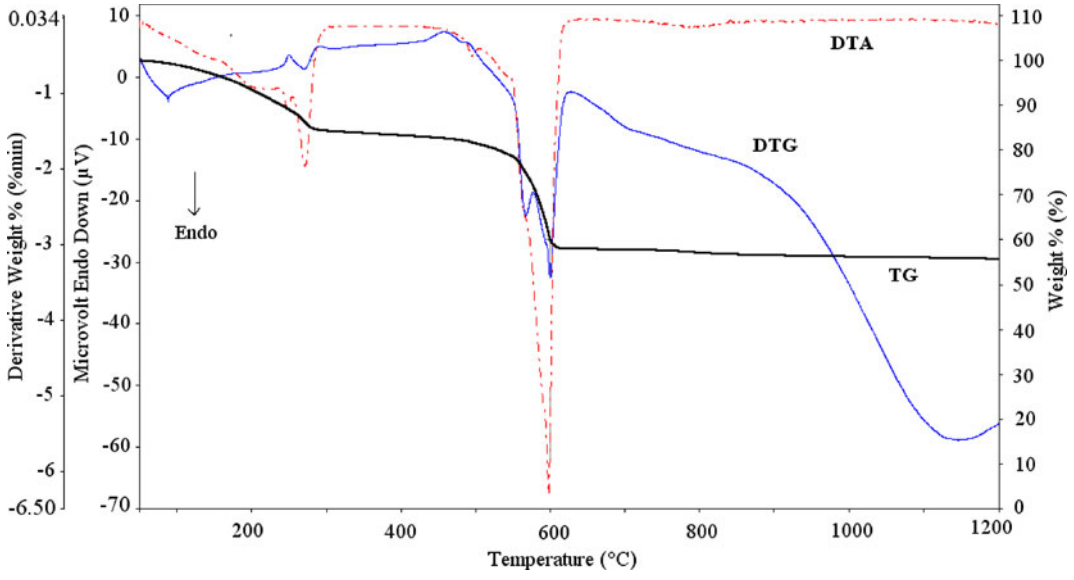

Figure 1. DTA/TG curves of phosphor.

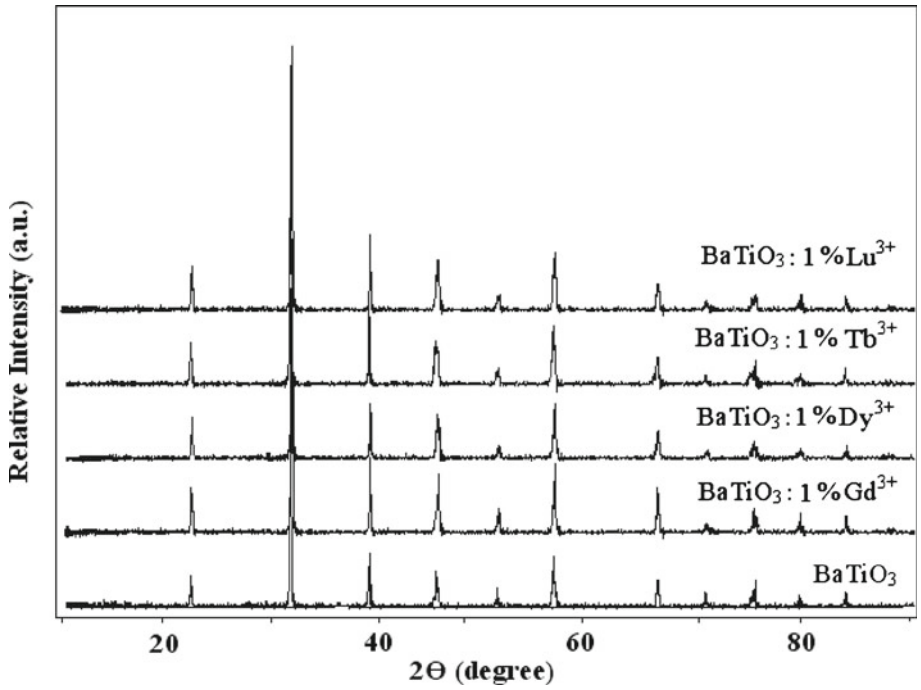

Figure 2. XRD pattern of phosphors calcined at 1000 °C.

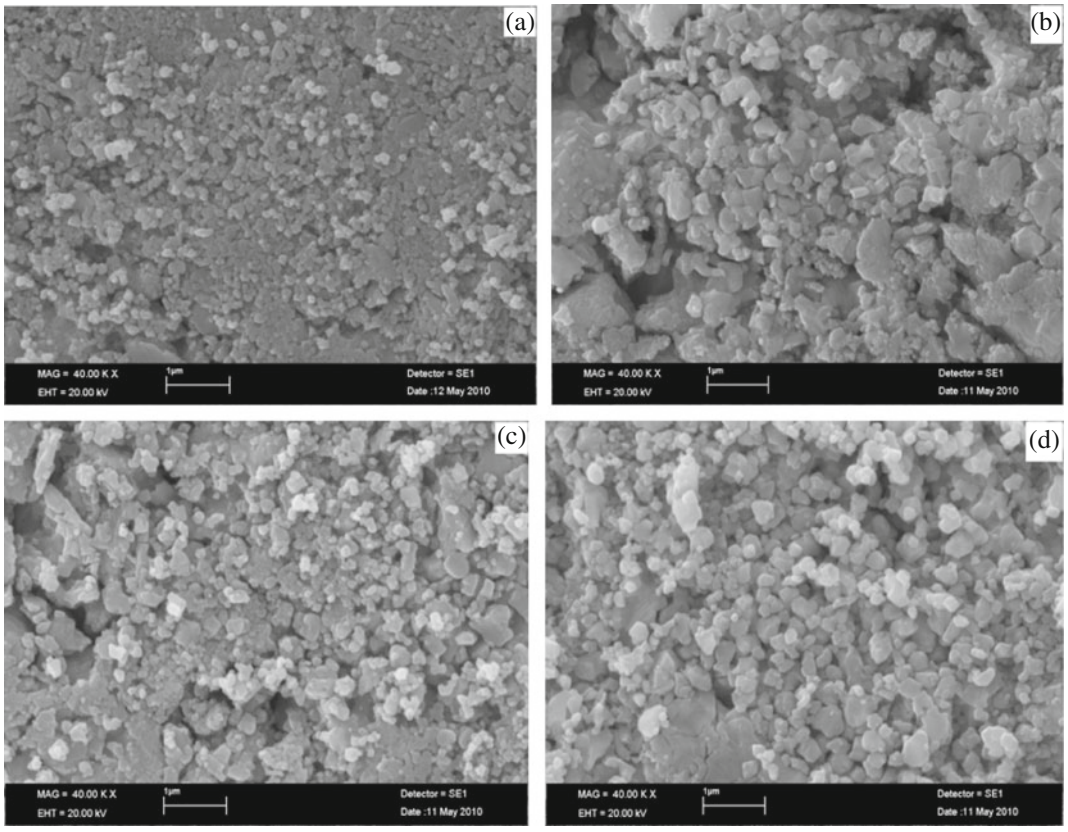

Figure 3. SEM images of (**a**) $BaTiO_3$:Gd^{3+}, (**b**) $BaTiO_3$:Dy^{3+}, (**c**) $BaTiO_3$:Tb^{3+} and (**d**) $BaTiO_3$:Lu^{3+} phosphors.

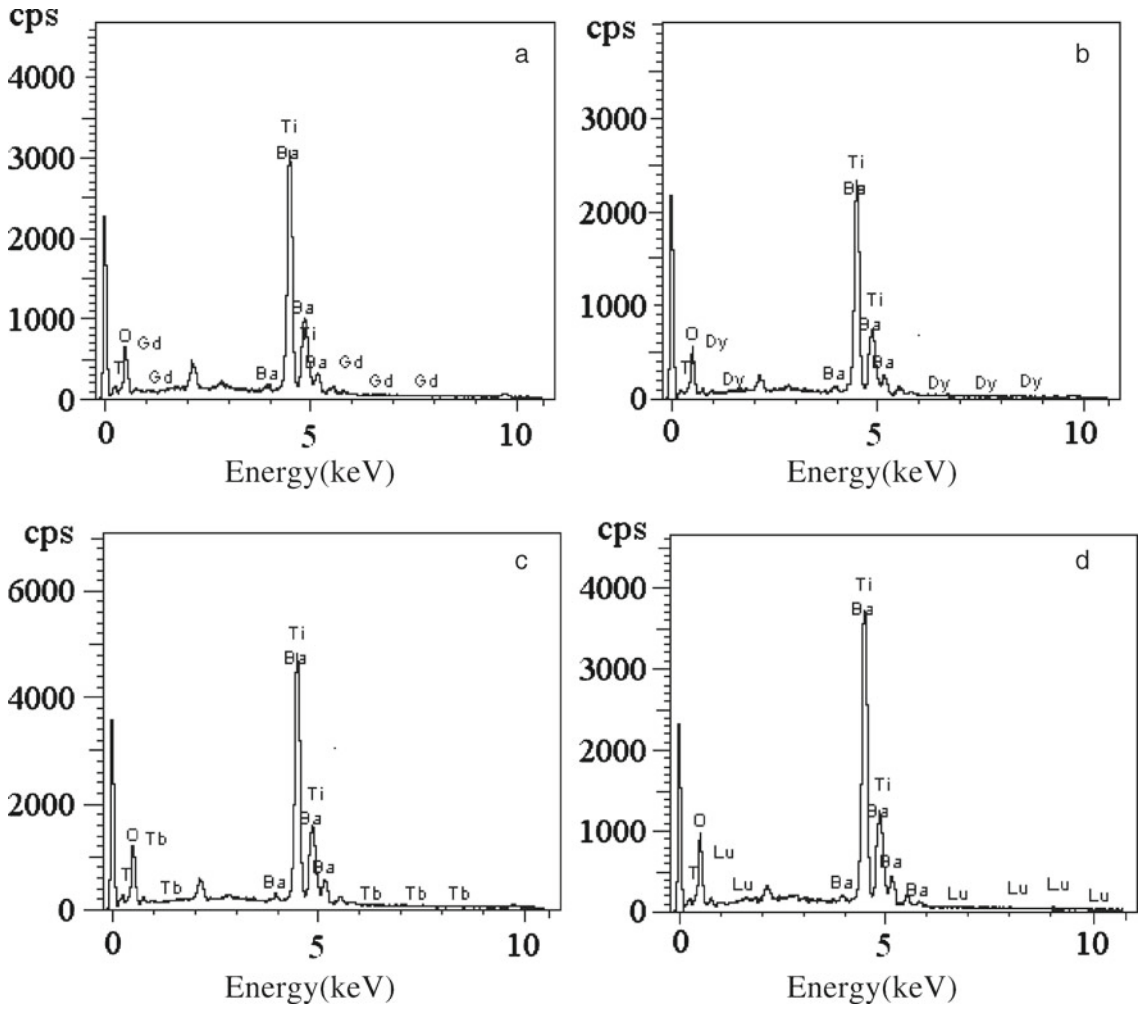

Figure 4. EDX analysis of (**a**) $BaTiO_3$:Gd^{3+}, (**b**) $BaTiO_3$:Dy^{3+}, (**c**) $BaTiO_3$:Tb^{3+} and (**d**) $BaTiO_3$:Lu^{3+} phosphors.

Table 1. EDX analysis results of phosphors.

	Theoretical				Experimental			
Phosphor	Ba	Ti	O	Rare earth	Ba	Ti	O	Rare earth
$BaTiO_3$	58·88	20·53	20·60	—	58·34	20·18	21·48	—
$BaTiO_3$:1%Gd^{3+}	58·49	20·39	20·45	0·67	59·53	20·78	18·82	0·87
$BaTiO_3$:1%Dy^{3+}	58·48	20·39	20·44	0·69	60·05	20·48	18·68	0·79
$BaTiO_3$:1%Tb^{3+}	58·49	20·39	20·44	0·68	61·51	19·10	18·80	0·59
$BaTiO_3$:1%Lu^{3+}	58·44	20·38	20·43	0·75	58·75	20·30	20·09	0·86

intensity of $BaTiO_3$ phosphor; $BaTiO_3$: Gd^{3+}, in particular, show the strongest absorption among the systems. This is due to the fact that doped Gd^{3+} ions caused an increase in the intensity of radiation band of the host crystal by forming defect centres in the host crystal.

It was determined that the characteristic $^4F_{9/2} \rightarrow ^6H_{13/2}$ electronic transition of the Dy^{3+} ion at 574 nm which overlapped with the radiation band of the host crystal took place as a result of the excitation process applied at 279·5 nm to the substance formed through the doping of 1% mole Dy^{3+} ion into the $BaTiO_3$ compound (Jayasimhadri *et al* 2006).

It was observed that $BaTiO_3$:1%Gd^{3+} formed through the doping of 1% mole Gd^{3+} ion into the $BaTiO_3$ compound which was excited at 291 nm, that Gd^{3+} ions performed the $^8S_{7/2} \rightarrow ^6I_J (J = 7/2, 9/2, 11/2, \ldots)$ electronic transitions at 275 nm and this transition overlapped with the radiation band of the host crystal (Flores-Gonzales *et al* 2005).

It was also observed that the $BaTiO_3$: 1% mole Tb^{3+} system provided two radiation bands at 456 nm and 681 nm as a result of its excitation at 220 nm and severe radiation band at 456 nm corresponded to the characteristic $^5D_3 \rightarrow ^7F_4$ electronic transition of Tb^{3+} ion (Caldiño *et al* 2006).

Electronic transitions are not observed for Lu^{3+} ion as it has a $4f^{14}5d^06s^0$ configuration. By doping this ion, we aimed to ensure the formation of defect centres in the host crystal. On the other hand, it was determined that traps resulting from its doping into the $BaTiO_3$ crystal caused an increase in emission intensity. The phosphorescence properties of the ceramics are given in table 2.

The doping of 1% mole Dy^{3+}, 1% mole Gd^{3+} and 1% mole Lu^{3+} ion into the host crystal increased radiation intensity by 30, 200 and 65 units, respectively. It was observed that the radiation band of the new luminescent formed by doping 1% mole Tb^{3+} ion into the $BaTiO_3$ host crystal produced radiation bands in two different wavelengths at 452 nm and 681 nm separate from that at 567 nm wavelength.

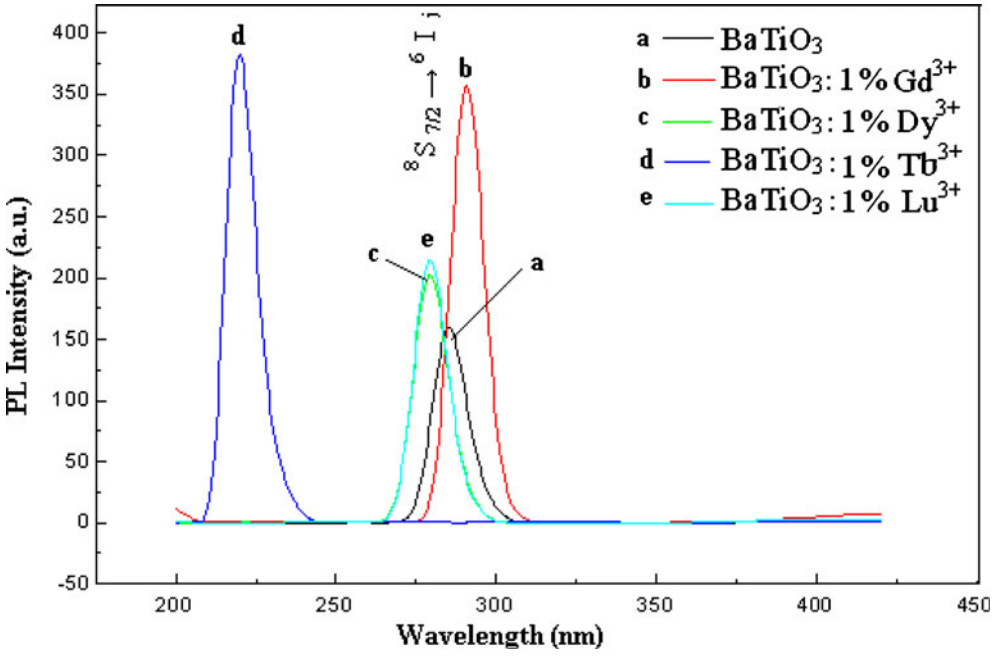

Figure 5. Excitation spectra of $BaTiO_3$ and $BaTiO_3$: RE (RE = Gd^{3+}, Dy^{3+}, Tb^{3+}, Lu^{3+}).

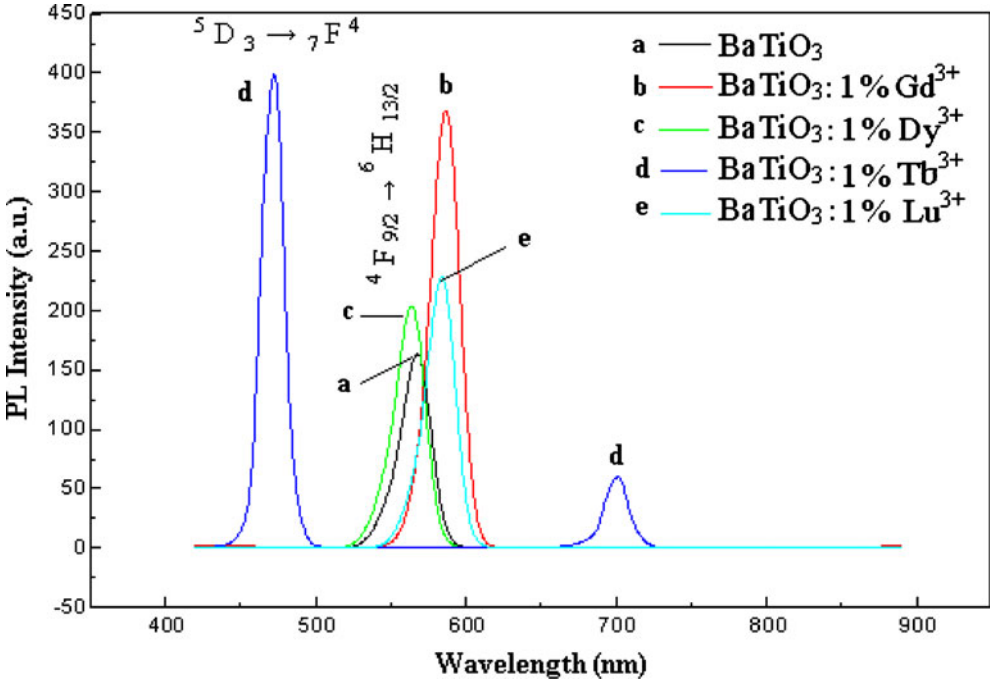

Figure 6. Emission spectra of $BaTiO_3$ and $BaTiO_3$: RE (RE = Gd^{3+}, Dy^{3+}, Tb^{3+}, Lu^{3+}).

Table 2. Phosphorescence properties of phosphors.

Phosphor	Radiation Intensity (a.u.)	Radiation colour	Radiation wavelength (nm)	Undoped-doped radiation difference
$BaTiO_3$	160	Yellow	567	—
$BaTiO_3$:1% Dy^{3+}	190	Yellow	564	30
$BaTiO_3$:1% Gd^{3+}	360	Yellow	587	200
$BaTiO_3$:1% Tb^{3+}	400–460	Orange	452–681	—
$BaTiO_3$:1% Lu^{3+}	225	Yellow	564	65

Table 3. Values of kinetic parameters of TL peaks of $BaTiO_3$: RE (RE = Gd^{3+}, Dy^{3+} and Tb^{3+}) samples determined by PS method.

Phosphor	T_M (°C)	E(eV)	b
$BaTiO_3$:1%Dy^{3+}	167	1	1·3
$BaTiO_3$:1%Gd^{3+}	95	0·2	2
$BaTiO_3$:1%Tb^{3+}	167	1·24	2

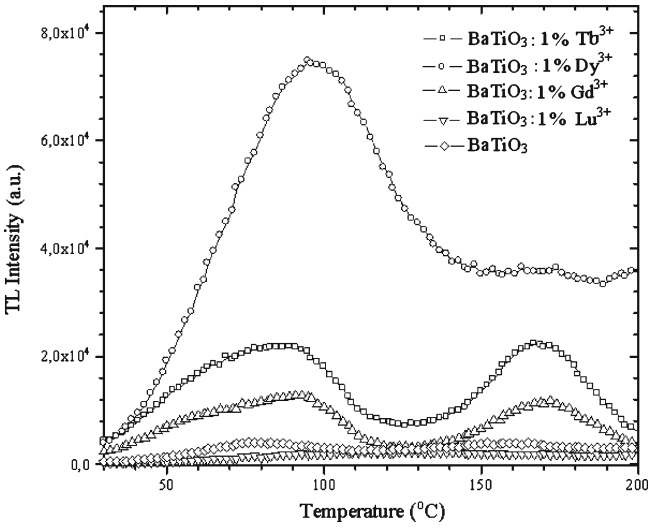

Figure 7. TL glow curves of $BaTiO_3$ and $BaTiO_3$: RE (RE = Gd^{3+}, Dy^{3+}, Tb^{3+}, Lu^{3+}) phosphors (D ≈ 36 Gy and β = 1°Cs^{-1}).

$BaTiO_3$:1%Gd^{3+}, in particular, shows strongest absorption among the systems.

The thermoluminescence (TL) properties of $BaTiO_3$ samples doped with Gd^{3+}, Dy^{3+}, Tb^{3+} and Lu^{3+} were also investigated. As seen from figure 7, TL glow curves of $BaTiO_3$ samples doped with Tb^{3+} and Gd^{3+} exhibit two glow peaks at around 95 and 167 °C and Dy^{3+} doped sample exhibits one strong glow peak at around 95 °C. Nevertheless, $BaTiO_3$ and $BaTiO_3$:Lu^{3+} phosphors do not show a TL characteristic.

Evaluation of kinetic parameters, i.e. the activation energy, E_a, of the traps involved in TL emission, the kinetic order, b and the frequency factor, s, associated with the glow peaks of thermally stimulated luminescence is one of the most studied subjects in the field of condensed matter physics. Because, a complete description of thermoluminescent characteristics of a TL material requires to obtain these parameters. Therefore, to form an opinion about the number of glow peaks and kinetic orders (b) of all individual glow peaks in the glow curve structure of $BaTiO_3$: RE (RE = Gd^{3+}, Dy^{3+} and

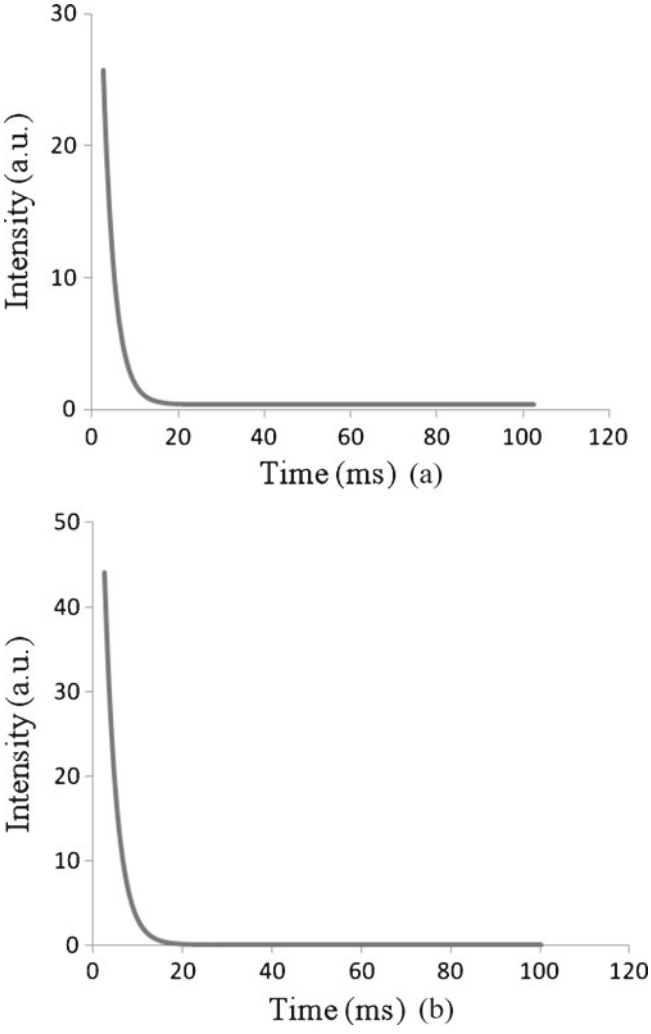

Figure 8. Decay curves of (**a**) $BaTiO_3$ and (**b**) $BaTiO_3$:Gd^{3+} phosphors.

Table 4. Life times for exponential, components of $BaTiO_3$, $BaTiO_3$:Gd^{3+}, $BaTiO_3$:Dy^{3+}, $BaTiO_3$:Tb^{3+} and $BaTiO_3$:Lu^{3+}phosphors.

Phosphor	Intensity (a.u)	Decay times, τ_1 (ms)
$BaTiO_3$	44·10	2·75
$BaTiO_3$:1%Gd^{3+}	25·74	2·66
$BaTiO_3$:1%Dy^{3+}	44·41	0·63
$BaTiO_3$:1%Tb^{3+}	15·76	0·51
$BaTiO_3$:1%Lu^{3+}	31·38	1·91

Tb^{3+}), the peak shape (PS) method was utilized in the current study. This method is based on the shape and full width at half maximum (FWHM $= T_2$–T_1) of a single glow peak and the values of E_a were determined by the modified PS method of Chen. According to this method, the b of a single peak is easily obtained by means of the geometric factor $\{\mu_g = (T_2–T_m)/(T_2–T_1)\}$ and μ_g changes with the order of kinetics, b, from $\approx 0{\cdot}42$ to $\approx 0{\cdot}52$, where these two limits correspond to first- and second-order kinetics, respectively (Chen and McKeever 1997). In the present case, average values of the parameters involved for the main dosimetric peaks are given in table 3.

The decay curves of $BaTiO_3$ and $BaTiO_3$:Gd^{3+} phosphors are shown in figures 8a and b. Decay times can be calculated by a curve fitting method based on the following single exponential equation:

$$I = A_1 \exp(-t/\tau_1) + C,$$

where I is phosphorescence intensity, A_1, C are constants, t the time, τ_1 the lifetime for the exponential components. The fitting results are given in table 4. The undoped $BaTiO_3$ phosphor shows much longer afterglow than the other phosphors which indicates that Gd^{3+}, Dy^{3+}, Tb^{3+} and Lu^{3+} ions do not play an important role in prolonging the afterglow.

4. Conclusions

In conclusion, $BaTiO_3$, $BaTiO_3$:Gd^{3+}, $BaTiO_3$:Dy^{3+}, $BaTiO_3$: Tb^{3+} and $BaTiO_3$:Lu^{3+} were synthesized by a modified solid-state reaction at 1000 °C. All phosphors were shown to have a tetragonal structure and the average diameter of the grain size of the material was in the range of 250–300 nm. The Gd^{3+} ion doped phosphor showed much stronger emission than other phosphors in a similar wavelength region but undoped $BaTiO_3$ phosphor shows much longer afterglow than the other phosphors. TL glow curves of $BaTiO_3$ samples doped with Tb^{3+} and Gd^{3+} exhibit two glow peaks at around 95 and 167 °C and Dy^{3+} doped sample exhibits one strong glow peak at around 95 °C. However, $BaTiO_3$ and $BaTiO_3$:Lu^{3+} phosphors do not show a TL characteristic.

Acknowledgements

The authors would like to thank Vural E. Kafadar, Gaziantep University, for his help in calculating the TL kinetic parameters using a curve-fitting program. Erciyes University's Research Fund (BAP-FBY 09-861 2009) financially supported this work.

References

Bhargava R, Gallagher D and Hong X 1995 *Phys. Rev. Lett.* **72** 416
Caldiño U, Speghini A and Bettinelli M 2006 *J. Phys. Condens. Matter* **18** 3499
Chen R and McKeever S W S 1997 *Theory of thermoluminescence and related phenomena* (Singapore: World Scientific)
Clabau F, Rocquefelte X and Jobic S 2005 *Chem. Mater.* **17** 3904
Clabau F, Rocquefelte X, Le Mercier T, Deniard P, Jobic S and Whangbo M H 2006 *Chem. Mater.* **18** 3212
Flores-Gonzales M A, Louis C, Bazzi R and Ledoux G 2005 *Appl. Phys.* **A81** 1385
Jayasimhadri M, Moorthy L R, Kojima K and Norikowada K Y 2006 *J. Phys. D: Appl. Phys.* **39** 635
Jia D, Meltzer R S, Yen W M, Jia W and Wang X 2002 *Appl. Phys. Lett.* **80** 1535
Lehmann O, Kompe K and Haase M 2004 *J. Am. Chem. Soc.* **126** 14935
Liu G K, Zhuang H Z and Chen X Y 2002 *Nano. Lett.* **2** 535
Liu G K, Chen X Y, Zhuang H Z, Li S and Niedbala R S 2003 *J. Solid State Chem.* **171** 123
Liu Y L, Lei B F and Shi C S 2005 *Chem. Mater.* **17** 2108
Matsuzawa T, Aoki Y, Takeuchi N and Murayama Y 1996 *J. Electrochem. Soc.* **143** 2670
Meltzer R S, Feofilov S P, Tissue B M and Yuan H B 1999 *Phys. Rev.* **B60** 14012
Meltzer R S, Yen W M, Zheng H, Feofilov S P and Dejneka M J 2002 *Phys. Rev.* **B66** 224202
Qiu J R, Gaeta A L and Hirao K 2001 *Chem. Phys. Lett.* **333** 236
Ruza E, Reyher H J, Trokss J and Wöhlecke M 1998 *J. Phys. Condens. Matter* **10** 4297
Shionoya S and Yen W M 1999 *Phosphors handbook* (New York: CRC Press)
Tissue B M 1998 *Chem. Mater.* **10** 2837
Williams D K, Bihari B, Tissue B M and McHale J M 1998 *J. Phys. Chem.* **B102** 916
Wuister S F, Donega C M and Meijerink A 2004 *Phys. Chem. Chem. Phys.* **6** 1633
Yan C H, Sun L D, Liao C S, Zhang Y X, Lu Y Q and Huang S H 2003 *Appl. Phys. Lett.* **82** 3511